

Single-electron transistor as a charge sensor for semiconductor applications

David Berman

Department of Electrical Engineering and Computer Science, Massachusetts Institute of Technology, Cambridge, Massachusetts 02139

Nikolai B. Zhitenev and Raymond C. Ashoori

Department of Physics, Massachusetts Institute of Technology, Cambridge, Massachusetts 02139

Henry I. Smith^{a)}

Department of Electrical Engineering and Computer Science, Massachusetts Institute of Technology, Cambridge, Massachusetts 02139

Michael R. Melloch

Department of Electrical Engineering and Computer Science, Purdue University, West Lafayette, Indiana 47907

(Received 6 June 1997; accepted 5 August 1997)

We describe the use of aluminum single-electron transistors (SETs) to measure, with extremely high sensitivity, the fluctuation of charge in semiconductor quantum dots. Our method of fabricating SETs results in excellent reliability and reproducibility. © 1997 American Vacuum Society. [S0734-211X(97)08706-4]

I. INTRODUCTION

Recently, single-electron transistors (SETs) have gained renown for their exceptional sensitivity to charge. Some of the first uses of SETs as charge sensors involved experiments with mesoscopic devices.^{1,2} These measurements require sufficient sensitivity to detect movements of charge equivalent to a fraction of an electron. In order to be able to perform such experiments, a highly reliable and reproducible fabrication process is necessary. In this article, we present our fabrication method and show some experimental results utilizing an Al/Al₂O₃/Al SET to measure charge on a semiconductor quantum dot.

II. SET FABRICATION

In the fabrication of conventional devices, one generally tries to achieve a resist profile with vertical sidewalls. This permits dense packing and is also desirable for various processing steps, such as metal liftoff. In contrast, SET fabrication employs the double-angle evaporation sequence, shown in Fig. 1, which requires a well-controlled undercut of the resist.

As in the original work of Fulton and Dolan,³ patterning is done by electron-beam lithography in a bilayer resist. We use a beam energy of 40 keV and a current of 20 pA, which provides a beam diameter of <20 nm. The bottom layer of the resist is a copolymer of polymethylmethacrylate (91.5%) and polymethacrylic acid (8.5%) (PMMA, PMAA), which is 450-nm-thick.⁴ After deposition, this layer is uniformly exposed with 220 nm ultraviolet (UV) radiation at a power density of 1 mW/cm² for a controlled period of time.⁵ A 50-nm-thick layer of 950 000 molecular weight PMMA⁶ is then deposited on top.

The amount of UV exposure of the bottom layer significantly affects the pattern profile in the resist. Figure 2 shows scanning-electron micrographs of line profiles for 0, 2, 3, and 4 min of UV exposure. The undercut, measured as the line width in the bottom resist layer, varies from 100 nm for no UV exposure of the bottom layer to 550 nm for a 4 min UV exposure. We selected the process parameters corresponding to an undercut of 350 nm, achieved with a 3 min exposure.

Electron-beam evaporation is used after pattern definition to deposit two separate 30-nm-thick aluminum layers. The tunnel junctions are made by forming a small overlap between two aluminum lines as depicted in the schematic in Fig. 1. The tunnel barrier consists of a thin aluminum oxide that is grown on the first layer by introducing a controlled amount of oxygen (50 mTorr for about 10 min) into the sample chamber after the first evaporation. The resistance of a tunnel junction is determined by the thickness of the oxide, which is in turn determined by the amount of oxidation. To achieve the proper tunnel junction resistance, we control the oxygen pressure and the period of time. The result is repeatable to within 10% and is shown in Fig. 3. This dependence is best described as a polynomial:

$$R = (3.7 \times 10^{-5}) P^3, \quad (1)$$

where R is the tunnel junction resistance in $M\Omega$, and P is the oxygen pressure in mTorr.

III. SET OPERATION

Figure 4 is a scanning-electron micrograph of a SET. The central island is coupled to the source and drain electrodes through two small tunnel junctions. In addition to presenting a resistance to the flow of electrons, the tunnel junctions have a capacitance, determined by the area of the overlap and the thickness of the oxide layer. The total capacitance of the central island is determined primarily by the tunnel junc-

^{a)}Electronic mail: hismith@nano.mit.edu

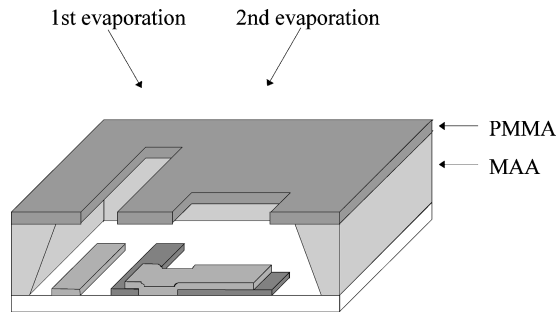


FIG. 1. Schematic of the double-angle evaporation process. Thickness of the MAA copolymer layer is 450 nm. Thickness of the PMMA layer is 50 nm. The two aluminum evaporations are performed at angles of $\pm 10^\circ$ to the normal. Oxygen is introduced into the chamber between evaporations for 10 min at a pressure of 50 mTorr to create the tunnel barriers.

tion capacitance. For optimal performance of the SET, the total island capacitance must be minimized, i.e., the area of the tunnel junctions must be as small as possible. We achieve tunnel junction area of $\sim 70 \times 70$ nm. The total central island capacitance in our devices is about 200×10^{-18} F. The operating temperature must be < 1 K, because the relation

$$k_B T \ll e^2 / 2C \quad (2)$$

must be satisfied, where C is the total island capacitance.

The operation of the SET is based on the Coulomb blockade principle,⁷ illustrated in the current–voltage (I – V) plot of Fig. 5(a). The flat portion of this curve signifies that a

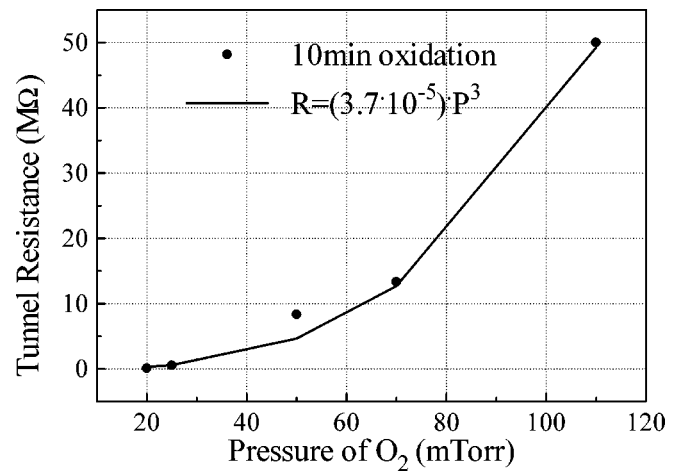


FIG. 3. Dependence of the tunnel junction resistance on the oxygen pressure for a 10 min oxidation.

finite V_{ds} is needed to overcome the Coulomb barrier. The width of this flat portion is periodically modulated by the gate voltage.

For fixed V_{ds} bias, the current through the SET exhibits a periodic dependence on the gate voltage, shown in Fig. 5(b). To maximize the amplitude of this variation, the source-drain voltage bias is adjusted to the value shown by the arrow in Fig. 5(a), i.e., $V_{ds} \cong 0.4$ mV.

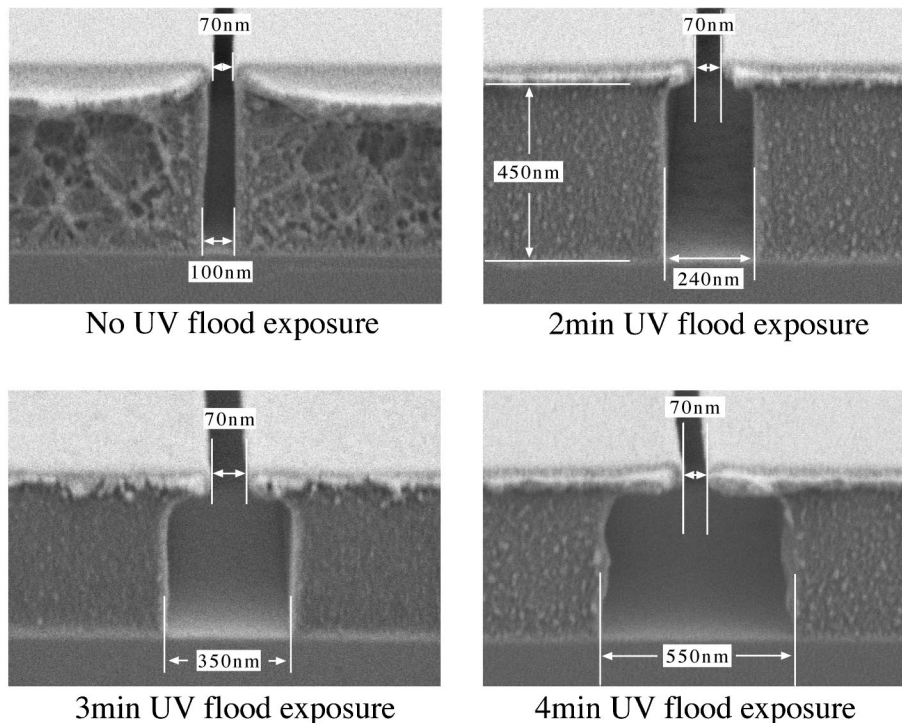


FIG. 2. Effect of varying the UV exposure of the bottom resist layer on the cross-sectional profile. A 3 min UV flood exposure is used in the SET fabrication process.

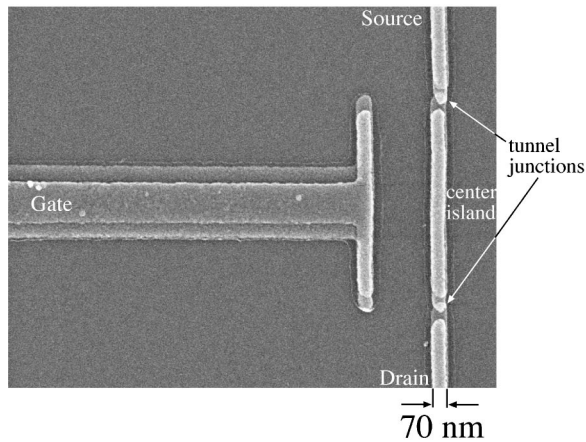


FIG. 4. Scanning-electron micrograph of an aluminum SET made with the double-angle evaporation process.

IV. CHARGE SENSING EXPERIMENT

We have fabricated a metal SET along with other leads on top of a GaAs/AlGaAs heterostructure with a two-dimensional electron gas (2DEG) 100 nm below the surface. Figure 6 shows a scanning-electron micrograph of the structure. By applying a negative potential to the metal leads with respect to the 2DEG, we deplete the electrons below, and create a small, isolated puddle of electrons in the 2DEG. We use the SET to study charge fluctuations on this puddle, identified as the “quantum dot” in Fig. 6.

The quantum dot is coupled to source and drain leads through two quantum point contacts. We can vary the resistance of these point contacts over a wide range by changing the potential on the metal leads. Ohmic contacts to the 2DEG allow us to flow and measure current through the quantum dot.

We have designed this structure so that the central island of the SET is located very close the quantum dot in the 2DEG. This guarantees that the capacitive coupling between the SET and the quantum dot is strong. As a result, the current through the SET is strongly modulated by the charge on the quantum dot. We achieved a charge sensitivity of $10^{-5} e/(\text{Hz})$ which matches the best numbers of experiments with SET charge amplifiers.^{8,9} This was determined by applying a signal of 1×10^{-3} electrons on the gate of the SET ($4 \mu\text{V}$ across a 50 aF gate capacitance) and measuring the signal in a 3 Hz bandwidth with a signal-to-noise ratio of 50.

V. MEASUREMENT

We perform the measurements by scanning the dc voltage, V_G , on the quantum dot gate, marked as “QD gate” in Fig. 6. Through a capacitance C_G , V_G polarizes the charge on the dot. We also apply a small ac signal to the same lead and use a lock-in amplifier to measure the current through the SET.

Figure 7 shows the dependence of the ac current through the SET on V_G . The signal that we measure is directly proportional to the slope of the SET transfer characteristic, such

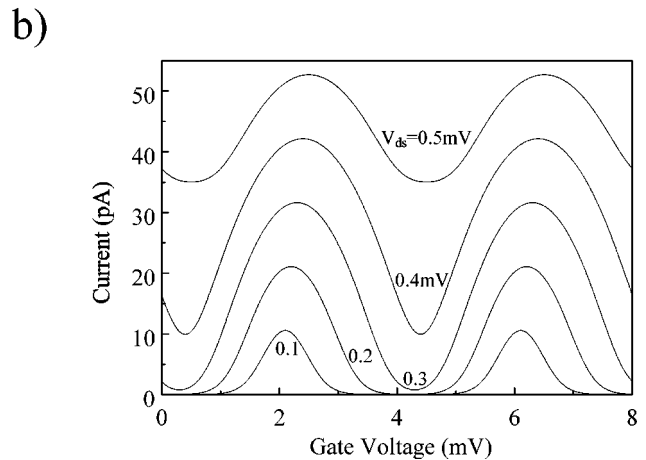
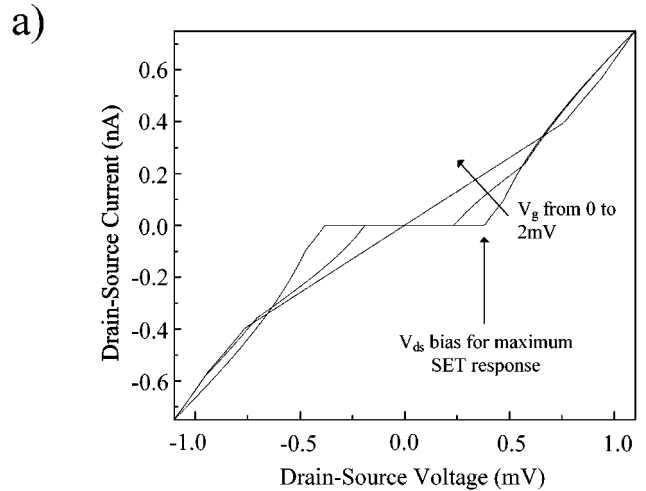


FIG. 5. Operational characteristics of the SET at 100 mK: (a) Source-drain I - N characteristics of the device for three different gate voltages: 0, 1, and 2 mV. The arrow shows the voltage bias for maximum response of the SET. $V_{ds} = E_c/e$. (b) Dependence of the current through the SET on the gate voltage for different source-drain voltage biases.

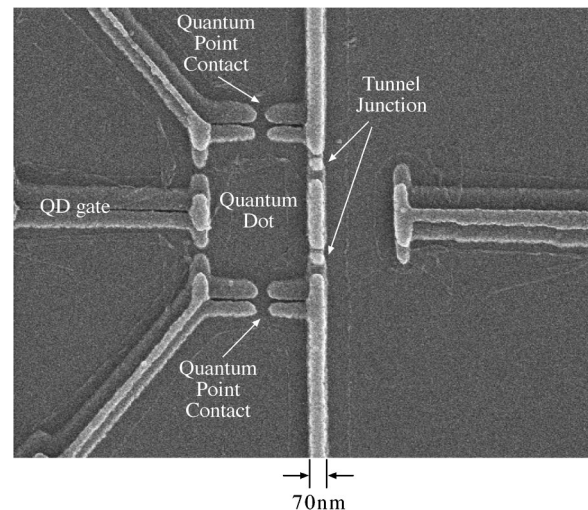


FIG. 6. Scanning-electron micrograph of the lead pattern on a GaAs/AlGaAs heterostructure, with a 2DEG 100 nm below the surface, used for a charge sensing experiment.

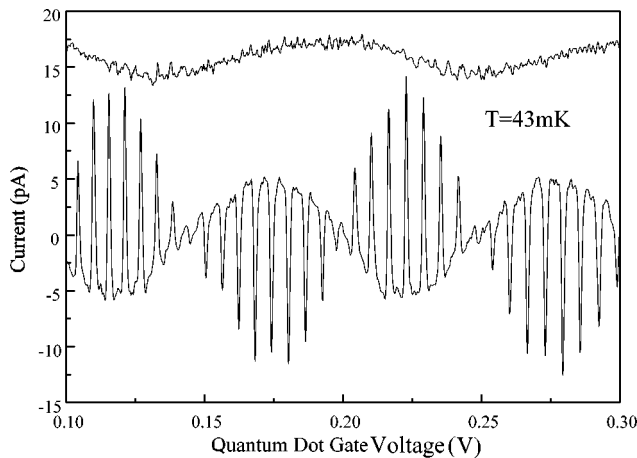


FIG. 7. Dependence of the current through the SET on the quantum dot gate voltage. Top curve, which has been offset for clarity shows the current through the SET without negative voltage bias applied to the metal leads, i.e., no quantum dot is formed in the 2DEG. Bottom curve: current through the SET with the quantum dot defined by applying proper negative potential to the metal leads. $T=43$ mK.

as in Fig. 5(b). Since the slope of the SET transfer characteristic oscillates between negative and positive values, depending on the charge that is present on the central island of the SET so does the signal that we measure. The top curve, which has been displaced for clarity, corresponds to the SET signal without negative voltage bias applied to the metal leads, i.e., no quantum dot is formed in the 2DEG. The bottom curve is the SET signal with the proper dc voltages applied to the leads to define the quantum dot in the 2DEG.

In the top curve, the situation is very simple; there is no quantum dot, and scanning the gate voltage simply changes the charge on the central island of the SET through a direct capacitance. When the quantum dot is formed, the situation changes significantly, i.e., the SET current is sensitive to charge fluctuations in the quantum dot.

Coulomb-blockade theory describes electron tunneling onto the quantum dot. Tunneling is suppressed, except for V_G values where

$$|C_G V_G| = e(n + 0.5) \quad (3)$$

is satisfied for integer values of n . At these values of V_G , the potential of the quantum dot is fixed by the electrons tunneling between the dot and the grounded ohmic contacts. Otherwise, the quantum dot potential is floating. As V_G is

scanned, the quantum dot periodically oscillates between being grounded and floating. The period is e/C_G . Since the quantum dot is located between the QD gate and the central island of the SET, the ac capacitance between them depends on the quantum dot potential. The oscillations of the dot potential cause this capacitance to oscillate as well. Since the ac current through the SET is directly proportional to this capacitance, is also goes through periodic oscillations.

Due to a small direct dc capacitance from the QD gate to the central island of the SET, it also goes through Coulomb blockade oscillations, but at much longer periods. This causes an overall envelope modulation of the SET signal, which is evident in the bottom curve of Fig. 7. The period of this envelope corresponds to the period of the oscillation in the top curve of Fig. 7, i.e., without the quantum dot.

VI. CONCLUSION

We have described improvements to the double-angle evaporation process for fabricating SETs in aluminum. Using a SET we have measured the charge on a quantum dot, attaining a sensitivity of $10^{-5} e/\sqrt{\text{Hz}}$.

ACKNOWLEDGMENTS

This work was supported by DARPA, the Joint Services Electronics Program, the Office of Naval Research and NSF-DMR.

¹P. Lafarge, H. Pothier, E. R. Williams, D. Esteve, C. Urbina, and M. H. Devoret, *Z. Phys. B* **85**, 327 (1991).

²D. Berman, R. C. Ashoori, and H. I. Smith, in *Proceedings of the International Conference on Quantum Devices and Circuits* (Imperial College Press, Alexandria, Egypt, 1996), p. 217.

³T. A. Fulton and G. J. Dolan, *Phys. Rev. Lett.* **59**, 109 (1987).

⁴Copolymer of polymethylmethacrylate (91.5%), and polymethacrylic acid (8.5%), is in an 11% solution in 2-ethoxyethanol from Microlithography Chemical Corp., Newton, MA. It is spun at 5 kRPM for 45 s, then baked at 125 °C for 30 min. The resulting thickness is 450 nm.

⁵L. Ji, P. D. Dresselhaus, S. Han, K. Lin, W. Zheng, and J. E. Lukens, *J. Vac. Sci. Technol. B* **12**, 3619 (1994).

⁶The 950 000 molecular weight PMMA is in a 2% solution in Anisole from Microlithography Chemical Corp., Newton, MA. It is spun at 5 kRPM for 45 s, then baked at 170 °C for 30 min. The resulting thickness is 50 nm.

⁷D. V. Averin and K. K. Likharev, in *Mesoscopic Phenomena in Solids*, edited by B. L. Altshuler, P. A. Lee, and R. A. Webb (North-Holland, Amsterdam, 1991), p. 173.

⁸E. H. Visscher, J. Lindeman, S. M. Verbrugh, P. Hadley, and J. E. Mooij, *Appl. Phys. Lett.* **68**, 2014 (1996).

⁹J. Pettersson, P. Wahlgren, P. Delsing, D. B. Haviland, T. Claeson, N. Rorsman, and H. Zirath, *Phys. Rev. B* **53**, R13 272 (1996).